0888-8809/02/$15.00/0
Printed in U.S.A.

Molecular Endocrinology 16(3):621–629

TASK-3 Dominates the Background Potassium Conductance in Rat Adrenal Glomerulosa Cells

GÁBOR CZIRJÁK AND PÉTER ENYEDI

Department of Physiology, Semmelweis University of Medicine, Budapest H-1444, Hungary

In a preceding study we showed that the highly negative resting membrane potential of rat adrenal glomerulosa cells is related to background potassium channel(s), which belong to the two-pore domain channel family. TWIK-related acid-sensitive K^+ channel (TASK-1) expression was found in glomerulosa tissue, and the currents elicited by injection of glomerulosa mRNA (I_{glom}) or TASK-1 cRNA (I_{TASK-1}) showed remarkable similarity in *Xenopus laevis* oocytes. However, based on the different sensitivity of these currents to acidification, we concluded that TASK-1 may be responsible for a maximum of 25% of the weakly pH-dependent glomerulosa background K^+ current. Here we demonstrate that TASK-3, a close relative of TASK-1, is expressed abundantly in glomerulosa cells. Northern blot detected TASK-3 message in adrenal glomerulosa, but not in other tissues. Quantitative RT-PCR experiments indicated even higher mRNA expression of TASK-3 than TASK-1 in glomerulosa tissue. Similarly to the glomerulosa background current, the current expressed by injection of TASK-3 cRNA (I_{TASK-3}) was less acid-sensitive than I_{TASK-1}. Ruthenium red in the micromolar range inhibited I_{glom} and I_{TASK-3}, but not I_{TASK-1}. Like I_{TASK-1}, I_{TASK-3} was inhibited by stimulation of AT1a angiotensin II receptor coexpressed with the potassium channel. The high level of expression and its pharmacological properties suggest that TASK-3 dominates the resting potassium conductance of glomerulosa cells. (*Molecular Endocrinology* 16: 621–629, 2002)

POTASSIUM CHANNELS CONTROLLING the membrane potential of adrenal glomerulosa cells play a pivotal role in the regulation of aldosterone production. Different sets of channel types are the major determinants of the membrane potassium conductance under resting and stimulated conditions. The depolarization-activated [delayed rectifier (1) and transient, A-type (2, 3)] K^+ channels and also the Ca^{2+}-activated (BK, maxi) K^+ channel (4, 5) were found previously to ensure the repolarizing currents during stimulation. However, the molecular entities responsible for the robust resting potassium conductance emerge at present. In principle, inwardly rectifying and background K^+ currents are the major candidates for inducing the negative resting membrane potential. Formerly single-channel events of inwardly rectifying K^+ channels were detected in glomerulosa membrane patches (1), but the inwardly rectifying and Ba^{2+}-sensitive macroscopic K^+ current characteristic for this channel type has never been reported in glomerulosa cells. More recently, background (leak) K^+ currents were described and suggested to have the primary role in the generation of the negative resting membrane potential in rat adrenal glomerulosa cells (5, 6). These results were confirmed also by our electrophysiological studies (7). In addition, we tried to resolve which channel(s) were responsible for the background current at the molecular level (7). Considering the biophysical and pharmacological properties of the two-pore domain (2P) potassium channel family, we searched for the presence of these channels in glomerulosa tissue.

In our preceding study we demonstrated high level expression of TWIK-related acid-sensitive K^+ channel (TASK-1) mRNA in the adrenal capsular tissue with Northern blot. It was verified that the mRNA of TASK-1 derives from glomerulosa cells by applying single-cell RT-PCR. Injection of glomerulosa mRNA into *Xenopus* oocytes evoked high K^+ conductance. Several pharmacological properties of I_{mRNA} and I_{TASK-1} (the K^+ currents expressed in *Xenopus* oocytes by injecting glomerulosa mRNA or TASK-1 cRNA, respectively) were identical. Furthermore, coinjection of an antisense oligonucleotide designed to anneal to the 5′-end of the TASK-1 coding region prevented the expression of I_{mRNA} specifically and almost completely. However, I_{TASK-1} was more sensitive to extracellular (EC) acidification than I_{mRNA}, which suggested that the contribution of I_{TASK-1} to I_{mRNA} could be 25% at maximum (somewhat contradictory to the antisense results) (7).

Recent molecular cloning uncovered additional mammalian 2P potassium channels (for review see Ref. 8). Members of the 2P K^+ channel family have four transmembrane segments and two potassium channel pore-forming domains. Apart from the distinctive topology, they are distantly related at the amino acid level. They have different expression patterns and regulatory mechanisms. With the only exception of TWIK-2 (9), all the functionally expressed 2P channels induce noninactivating background K^+ currents.

In this study we examined whether the recently described 2P channels, TASK-2 (10) or TASK-3 (11, 12),

Abbreviations: EC, Extracellular; 2P, two-pore; RR, ruthenium red; TASK, TWIK-related acid-sensitive K^+ channel.

the closest structural relative of TASK-1, were present in glomerulosa tissue, and whether their expression could be responsible for the previously observed difference between the pharmacology of glomerulosa and TASK-1 currents. Our data indicate that TASK-3 is expressed in high abundance in glomerulosa tissue, and its pharmacology gives an explanation not only for the previously observed discrepancy between I_{mRNA} and I_{TASK-1}, but suggests that TASK-3 is responsible predominantly for the negative resting membrane potential of glomerulosa cells. We show, moreover, that TASK-3 is prone to be inhibited by angiotensin II; thus it may also be involved in the angiotensin II-induced depolarization of glomerulosa cells.

RESULTS

Expression of TASK-3 mRNA in the Adrenal Zona Glomerulosa

RT-PCR was performed from rat adrenal capsular (glomerulosa) tissue total RNA with the T3s and T3a primers designed on the basis of the recently published sequence information of the 2P potassium channel, TASK-3 (11). The amplified DNA fragment had the expected length (776 bp). Specificity of the PCR product was verified by sequencing, which indicated that the TASK-3 channel is expressed in glomerulosa cells. To estimate the relative abundance of TASK-1, TASK-2, and TASK-3 mRNA in glomerulosa tissue, we used the degenerate T123s and T123a primer pair to amplify the cDNA fragments of these channels simultaneously by RT-PCR. Digestion of the heterogenous product with specific restriction enzymes for different TASK channels indicated similarly high abundance of TASK-1 and TASK-3 (47 ± 2% and 46 ± 3%, respectively), whereas TASK-2 represented only a minor fraction (9 ± 3%) (Fig. 1A, n = 3 independent glomerulosa RNA preparations).

Because the different efficiency of amplification of the three TASK channels by the degenerate T123s and T123a oligonucleotides could not be excluded, competitive PCR experiments were performed for more quantitative assessment. Competitive templates were designed by spoiling unique restriction enzyme sites in the cDNAs of the three TASK channels. Different, known amounts of the competitive templates were mixed with a fixed amount of reverse transcription reaction from glomerulosa RNA, and radioactive PCR product was amplified with primers annealing to the competitive template, flanking the mutated restriction

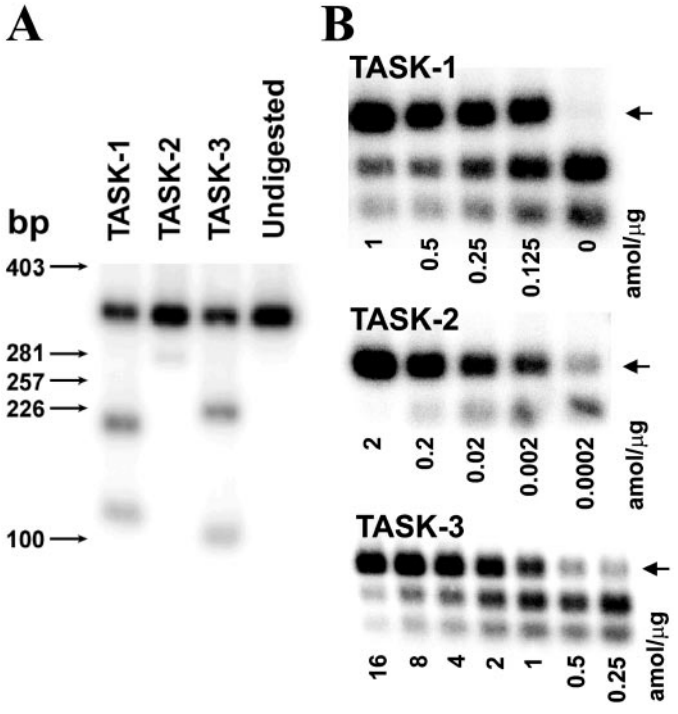

Fig. 1. Determination of the mRNA Expression Levels of TASK-1, TASK-2, and TASK-3

A, The radioactive PCR products amplified from adrenal capsular total RNA with the degenerate T123s and T123a primers were digested with the TASK-1 specific *Nco*I, the TASK-2-specific *Pvu*II, the TASK-3-specific *Eco*91I or incubated without any restriction enzyme, respectively (representative of three experiments.) B, Representative TASK-1, TASK-2, and TASK-3 competitive PCR experiments. The digestion-resistant bands (which are the products from the competitive template) are marked with *arrows*. The reactions contained fixed amounts of the RT product, and various amounts of the competitive template as indicated for each reaction in 10^{-18} mol (template strand)/μg RNA. The digested TASK-2 fragments have about equal size, and therefore show only one band.

enzyme site. Although the wild-type PCR products originating from the reverse transcription reaction were cleaved by the restriction enzyme, the mutant PCR products deriving from the competitive template remained unaltered. Thus, the unknown quantity of the template from the reverse transcription reaction could be compared with the known amount of the competitive template by measuring the radioactivity of the digested fragments and the digestion-resistant band (Fig. 1B). The TASK-1 quantity was $3.6 \pm 1.3 \times 10^{-19}$ mol of template strand/μg glomerulosa total RNA (n = 11 PCR). The TASK-2 expression was much smaller, less than 2×10^{-20} mol/μg in four independent experiments. The TASK-3 expression ($1.4 \pm 0.3 \times 10^{-18}$ mol/μg, n = 7 PCR) was significantly higher than the expression of TASK-1 ($P < 0.05$, *t* test).

The expression level of the TASK-3 mRNA in the adrenal glomerulosa was compared with that of other tissues by Northern blot. The radioactive probe corresponded to the unique C-terminal intracellular tail of the channel. A representative Northern blot, shown in Fig. 2 indicates that the specific (~3.9 kb) message was detected exclusively in the adrenal glomerulosa tissue.

Cloning of TASK-3

To compare TASK-3 with the glomerulosa potassium conductance expressed heterologously in *Xenopus* oocytes, the complete TASK-3 coding region was cloned from rat glomerulosa tissue. The 1,204-bp cDNA of the channel was amplified by RT-PCR and cloned into the *Xenopus* expression plasmid, pEXO. Sequencing our clone from both directions showed a difference from the published rat TASK-3 sequence (nucleotides 507–520 numbered from the start codon) corresponding to TLCLG instead of LVPW at the protein level. Therefore, an additional PCR product was amplified independently from the previous one, and its sequencing gave the same result. The corrected rat sequence [which is similar to the human amino acid sequence at this critical region (12)] was deposited to the GenBank (accession no. AF391084).

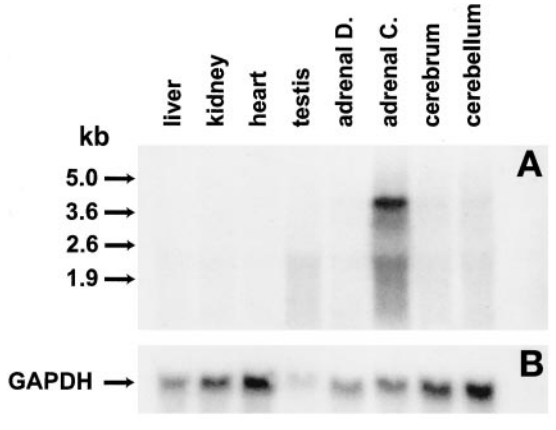

Fig. 2. Tissue Distribution of TASK-3 Transcripts in Rat Tissues

A, The expression of TASK-3 mRNA was analyzed by Northern blot. Each lane represents 10 μg total RNA from the tissues indicated (adrenal D, decapsular tissue; adrenal C, capsular tissue). Expression of TASK-3 mRNA was present in the adrenal capsular tissue (mainly glomerulosa) as a 3.9-kb band. *Arrows* indicate the position of RNA markers. B, For control the same blot was reprobed with glyceraldehyde-3-phosphate dehydrogenase cDNA.

Expression of TASK-3 and Pharmacological Comparison of I_{mRNA}, I_{TASK-1} and I_{TASK-3}

Injection of TASK-3 cRNA into *Xenopus* oocytes shifted their resting membrane potential toward more negative values (-91 ± 2 mV, n = 5). The potassium current responsible for this shift was measured at -100 mV by a two-electrode voltage clamp. The increase of the inward current on elevation of the EC $[K^+]$ from 2 mM to 80 mM can be regarded as an indication of the K^+ conductance of the plasma membrane. In oocytes expressing TASK-3, this increase of current (I_{TASK-3}) was several microamperes (14.9 ± 2.7 μAmp, n = 19), much larger than the 50–100 nAmp current increase in control (non-, or water-injected) oocytes. Therefore, I_{TASK-3} and its alteration by treatments could be measured similarly to I_{TASK-1} and I_{mRNA} (the currents expressed by injection of TASK-1 cRNA and glomerulosa mRNA, respectively) (7). In our preceding study we showed that Ba^{2+} (300 μM) and Cs^+ (3 mM) exerted voltage-dependent block of I_{mRNA} and I_{TASK-1}. TASK-3 was inhibited by the same concentration of these ions (Fig. 3.). Similarly to I_{TASK-1}, Ba^{2+} and Cs^+ caused voltage-dependent block of I_{TASK-3} in the hyperpolarized voltage range. The Ba^{2+} block developed slowly in time, but the steady state inhibition by Cs^+ was almost instantaneous. Under our experimental conditions the Ba^{2+} and Cs^+ inhibitory profiles of I_{TASK-1} and I_{TASK-3} were indistinguishable (not shown).

The formerly described major pharmacological difference between I_{mRNA} and I_{TASK-1} was their different acid sensitivity. Similarly to the K^+ conductance measured directly in glomerulosa cells (7), the pH sensitivity of the K^+ current induced by heterologous expression of glomerulosa mRNA in oocytes was weaker ($14.8 \pm 1.2\%$ inhibition, n = 9) than that of TASK-1 ($70.4 \pm 1.9\%$, n = 14), when the EC pH was reduced to 6.5 from 7.5. Therefore, the effect of pH on I_{TASK-1} and I_{TASK-3} was compared under identical conditions (Fig. 4). The pH sensitivity curves of TASK-1 and TASK-3 were similar, but the curve of TASK-3 was shifted to more acidic values [half-maximal inhibition at pH 6.8 (TASK-1) and pH 6.0 (TASK-3)]. Thus the inhibition of TASK-3 by the pH step from 7.5 to 6.5 fits well to the degree of inhibition of the glomerulosa current. The pH sensitivity of I_{mRNA} was evaluated also in a wider pH range. However, activation of an endogenous current of the oocyte by stronger acidification (pH 5–6) made the quantitative evaluation of I_{mRNA}

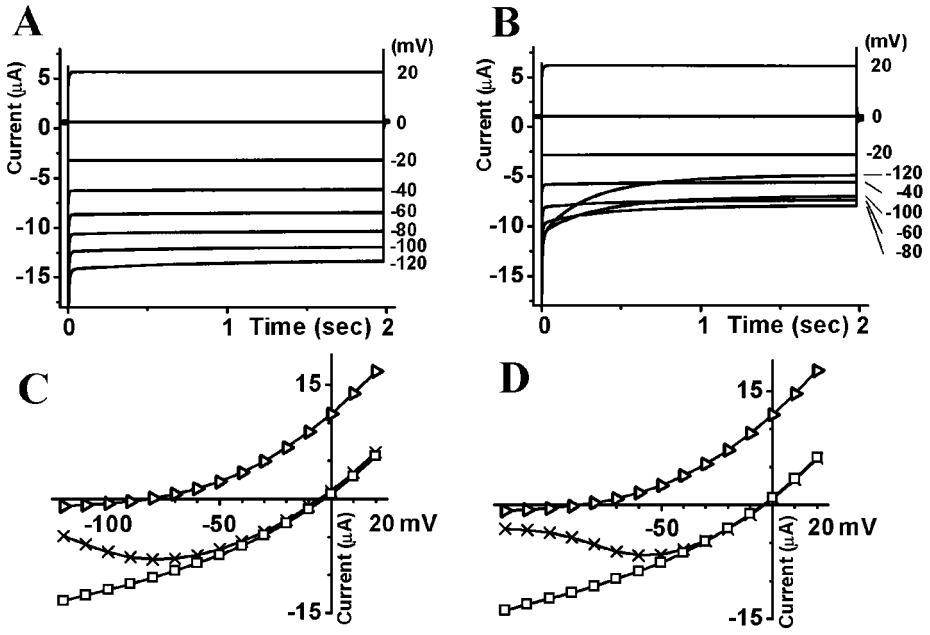

Fig. 3. Voltage-Dependent Inhibition of TASK-3 by Ba^{2+} and Cs^{+}

A, Control I_{TASK-3} currents elicited by voltage steps to the indicated membrane potentials from a holding potential of 0 mV in high (80 mM) EC $[K^{+}]$. B, Voltage-dependent inhibition by 300 μM Ba^{2+} in the same cell. (The protocol was the same as in panel A.) C, Steady-state current-voltage relationship measured at the end of the voltage steps in low (2 mM, ◁) and in high (80 mM) $[K^{+}]$ solutions in the presence (X) and in the absence (□) of 300 μM Ba^{2+}. D, Voltage-dependent inhibition by 3 mM Cs^{+} (X) in high $[K^{+}]$. [The same oocyte and the same protocol as in panel C. The low (◁) and high (□) potassium control curves were recorded again after the complete washout of Ba^{2+}.]

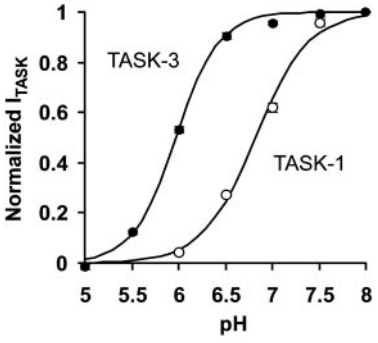

Fig. 4. pH Sensitivity of TASK-1 and TASK-3

Currents of oocytes expressing TASK-1 (*empty symbols*) or TASK-3 (*filled circles*) were measured at different pH values in high (80 mM) EC $[K^{+}]$ at −100 mV. The currents were corrected for the small nonspecific leak in 2 mM EC $[K^{+}]$ at −100 mV and normalized to the maximum at pH 8. Each *point* represents average of the normalized currents of five oocytes. In most cases *error bars* are smaller than *symbols*. Smooth curves were fitted according to Hill equations.

inhibition ambiguous. Increase of this endogenous current in noninjected oocytes at −100 mV has never exceeded 0.5 μAmp (n = 7). Therefore it did not influence the measurement of the pH sensitivity of TASK currents (amplitude of several microamperes) but could mask some of the inhibition of the smaller I_{mRNA}. Nevertheless, even with the activation of this current, substantial inhibition of I_{mRNA} was observed in some oocytes in the pH sensitivity range of TASK-3 (Fig. 5).

It was demonstrated by us that the cationic dye, ruthenium red (RR), depolarizes glomerulosa cells profoundly by inhibiting their background K^{+} conductance (16). Therefore, the effect of this drug was tested on I_{mRNA} in *Xenopus* oocytes. As anticipated, RR inhibited I_{mRNA} in the micromolar range (Fig. 6A). The inhibition evolved quickly, suggesting an EC site of action and it was reversible upon prolonged washout (not shown). The dose-response curve of RR was best fitted by a Hill equation in which RR did not induce complete inhibition of I_{mRNA}. According to this, the maximal inhibition was 75%, with a half-maximal effect at 0.6 μM. The Hill coefficient of 0.93 suggests that one RR molecule binds to one inhibited channel. RR proved to be a valuable pharmacological tool in evaluating the contribution of I_{TASK-1} and I_{TASK-3} to I_{mRNA}. It discriminates well between the closely related TASK-1 and TASK-3 (Fig. 6B); TASK-3 is inhibited by 68.8 ± 2.7% (n = 7) by 3 μM RR, whereas TASK-1 is not affected at all (0.7 ± 1.2%, n = 5). In accordance with the pH sensitivity data, this suggests that I_{mRNA} is dominated by TASK-3.

Angiotensin II Inhibits TASK-3

Oocytes heterologously expressing angiotensin II receptor respond to angiotensin II challenge with cal-

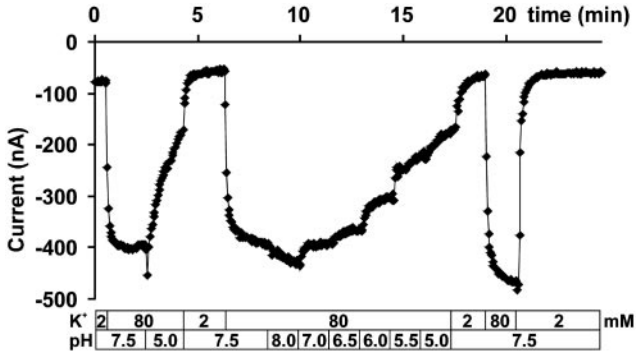

Fig. 5. Acidification Inhibits I_{mRNA}

Representative trace of an oocyte injected with glomerulosa mRNA. Currents were measured at the end of 300-msec voltage steps to −100 mV in every 3 sec in EC medium of different [K^+] and pH (as indicated *below* the curve).

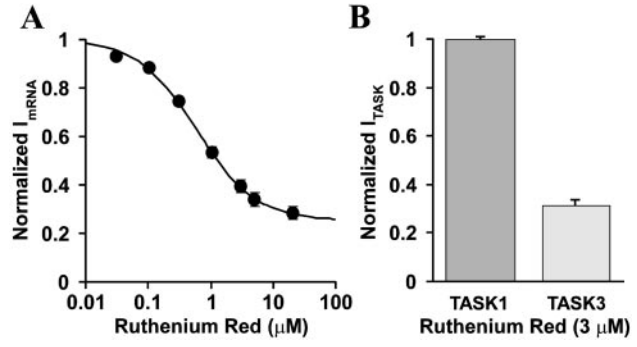

Fig. 6. RR Inhibits I_{mRNA} and TASK-3 But Not TASK-1

A, Concentration-dependent inhibition of I_{mRNA} by RR. (The applied RR concentrations were 0.03, 0.1, 0.3, 1, 3, 5, and 20 μM.) The currents were normalized to the value without RR. Each *point* represents average of the normalized currents of 10 oocytes. In most cases *error bars* are smaller than *symbols*. Incomplete inhibition was fitted by a modified Hill equation. B, Inhibition of TASK-1 (n = 5) and TASK-3 (n = 7) by 3 μM RR.

cium signal, which can be detected by following the activation of the endogenous Ca^{2+}-activated Cl^- channel. In oocytes coexpressing also background potassium channels, the K^+ current and the Ca^{2+}-activated Cl^- current ($I_{Cl,Ca}$) can be measured simultaneously and fairly separately, as it has been described previously (7, 17). Briefly, at −100 mV in high (80 mM) EC [K^+] the current consists of the robust K^+ influx predominantly, and activation of $I_{Cl,Ca}$ increases the inward current negligibly. However, at +20 mV (close to the K^+ equilibrium potential) $I_{Cl,Ca}$ is the major component of the outward current appearing upon receptor stimulation. Accordingly, the currents at −100 and +20 mV were measured in oocytes coexpressing TASK-3 and AT1a angiotensin II receptor (Fig. 7). Stimulation with angiotensin II (10 nM) inhibited I_{TASK-3} by 27.8 ± 1.7% (n = 15). Similarly to our previously reported results (7) angiotensin II evoked only a small inhibition of I_{mRNA}, whereas appearance of $I_{Cl,Ca}$ indicated that the angiotensin II receptor was expressed in response to injection of glomerulosa mRNA (not shown).

To test the receptor specificity of the TASK-3 inhibition, the effect of other receptors on the channel activity was examined. Stimulation of the endogenous lysophosphatidic acid receptor inhibited the potassium current in oocytes expressing TASK-3 (17.6 ± 3.3%, 0.5 μM lysophosphatidic acid, n = 8). Similarly, when the muscarinic M1 receptor was coexpressed with TASK-3, its stimulation with carbachol (1 μM) reduced the K^+ current by 44.8 ± 2.3% (n = 6).

DISCUSSION

In the present study we demonstrate that, in addition to TASK-1 (7), another member of the 2P potassium channel family, TASK-3, is expressed abundantly in adrenal glomerulosa cells. The TASK-3-specific message could be detected not only by RT-PCR, but we obtained a strong signal also by Northern blot with a probe corresponding to the unique C-terminal region of the channel. Previous attempts failed to detect TASK-3 mRNA with Northern blot in several tissues (under conditions that enabled the detection of TASK-1), leading to the conclusion that TASK-3 is expressed at very low levels if expressed at all (11). Our results

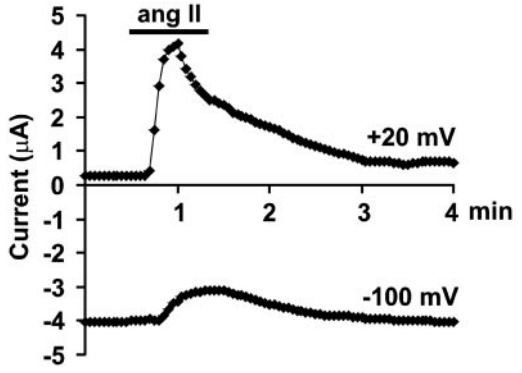

Fig. 7. Inhibition of TASK-3 by Angiotensin II

Currents of an oocyte coexpressing AT1a angiotensin II receptor and TASK-3 were measured during angiotensin II (10 nM) stimulation (as indicated by the *bar*) in high (80 mM) EC $[K^+]$. A voltage protocol comprising successive steps to −100 mV (300 msec), 0 mV (250 msec), and +20 mV (300 msec) was applied in every 3 sec from a holding potential of 0 mV. Currents at the end of the voltage steps to −100 and +20 mV were plotted as the function of time.

confirm these results respective to all tissues examined, except for the adrenal capsule, which showed a solid positive signal.

To estimate the relative quantity of mRNAs of different TASK channels in glomerulosa tissue, RT-PCR was performed with degenerate oligonucleotides, which annealed to conserved sequences of TASK-1 (15), TASK-2 (10), and TASK-3 (11). The proportion of TASK-1 and TASK-3 mRNA proved to be higher than that of TASK-2. Because the degenerate oligonucleotides may have amplified one or the other TASK channel preferentially, more reliable quantitative results were obtained; the mRNA expression levels of the three TASK channels were determined one by one by competitive PCR. These experiments demonstrated about 4-fold higher expression of TASK-3 than TASK-1, whereas TASK-2 mRNA was present at a far lower concentration. During the preparation of this paper the sequence of the fourth member of the TASK subfamily was published (18). However, TASK-4 conducts measurable current only above pH 9, which renders its physiological significance rather enigmatic.

With the aim of detailed analysis and comparison of the expressed I_{TASK-3} and I_{mRNA}, we took advantage of the published TASK-3 sequence (11) and amplified the coding region of the channel by RT-PCR from glomerulosa RNA. The PCR product was cloned and its sequence was determined. Apart from a minor difference, which probably results from some sequencing errors (a short frame-shifted fragment and three bases missing) in the previously published TASK-3 sequence deposited to the GenBank, our sequence turned out to be identical with the published one. The TASK-3 coding region was subcloned into a *Xenopus* expression plasmid and I_{TASK-3} was expressed and examined in the oocytes.

Inhibition of TASK-3 by acidification appears at lower pH than that of TASK-1. Accordingly, the approach (a pH step from 7.5 to 6.7) we used in our previous study to reveal the presence of TASK-1 in glomerulosa cells, also inhibited TASK-3, but only by 10–20%. This highly resembles the degree of inhibition of I_{mRNA} and of glomerulosa cell K^+ current by this pH step (7). We also found that the weakly pH-sensitive I_{mRNA} was inhibited specifically and almost completely by an antisense oligonucleotide designed to hybridize to the 5′-end of TASK-1 (7). However, the nucleotide sequences of rat TASK-1 and TASK-3 are identical in this region; accordingly the antisense inhibition could have manifested on both channels.

The polycationic dye RR is known to affect different Ca^{2+} transport-, and calcium-regulated processes (c.f. Ref. 19). It was shown to inhibit also Ca^{2+}-activated potassium currents (IK and BK) from the intracellular side, an effect interpreted as a probable interaction with the Ca^{2+}-binding sites of the channel protein (20). However, in addition to the Ca^{2+}-related processes, RR affects other ion transport mechanisms as well (21, 22). In a previous study we found that RR, when applied extracellularly, depolarized the adrenal glomerulosa cells by inhibiting the resting K^+ conductance (16). Accordingly, RR inhibited I_{mRNA} in the oocytes in the micromolar concentration range. Therefore we examined whether the candidates for the glomerulosa resting potassium current, I_{TASK-1} and I_{TASK-3} , were affected by RR. Our present results show that TASK-3 is highly sensitive to RR (3 μM exerts 70% inhibition) whereas the same concentration of the dye does not affect TASK-1 current at all. The strong inhibition of I_{mRNA} by RR confirms the major background potassium channel role of TASK-3 in glomerulosa cells. Although RR turned out to be an excellent tool for dissecting the relative contribution of the two TASK channels to I_{mRNA}, it was not specific enough to inhibit TASK-3 selectively in the glomerulosa cell. Formerly, RR was shown to reduce also the voltage-dependent Ca^{2+} currents of glomerulosa cells (16). Therefore, the effects of RR on the complex regulation of aldosterone production should be regarded carefully, because this drug also influences other important regulatory mechanisms in addition to the efficient inhibition of the background K^+ conductance (16).

Sensitivity of the glomerulosa cell to EC $[K^+]$ changes in the physiological range is regarded as a consequence of the depolarizing shift of the potassium equilibrium potential (E_K) (23–27). TASK-3 maintains highly negative resting membrane potential, thus allowing pronounced depolarization in a range, where the H subtype of the T type voltage-dependent Ca^{2+} channels [recently identified as the dominant low-voltage-activated Ca^{2+} channel in the glomerulosa cell (28)] may open. The significance of the low-voltage-activated mechanisms in the regulation of aldosterone production is well documented (23, 29), and they may influence other components having feedback also to

the membrane potential [*e.g*. stimulation of the sodium pump (30)].

We also demonstrated that TASK-3, expressed in *Xenopus* oocytes, is inhibited by AT_{1a} receptor stimulation. Although the TASK-3 inhibition by angiotensin II (28%) was smaller than the inhibition of TASK-1 [77% (Ref. 7)] in the oocyte, it should be pointed out that the glomerulosa K^+ current expressed in the oocytes (I_{mRNA}) showed also smaller inhibition by angiotensin II than the background K^+ current in the glomerulosa cell (7). This indicates that the degree of inhibition of the same channel may depend on the experimental system. In addition to the angiotensin II receptor, activation of the endogenous lysophosphatidic acid receptor and also the heterologously expressed M1 muscarinic receptor inhibited the TASK-3 current. Thus, similarly to TASK-1, the inhibitory mechanism of TASK-3 is not restricted to angiotensin II, but could be evoked by a wider range of receptors activating the Gq protein-PLC signaling pathway.

Although detailed analysis of the mechanism of regulation of TASK-3 was beyond the scope of this study, the deviation of the time courses of the calcium signal and the channel inhibition allows further speculation. Although the angiotensin II-induced Ca^{2+} signal (measured as calcium-activated chloride current in the oocyte) was rapidly reduced to a sustained phase after the initial peak, the TASK-3 inhibition remained nearly maximal during maintained stimulation. This apparent dissociation between the two effects suggests that the intracellular [Ca^{2+}] may not be the determining factor responsible for the TASK-3 inhibition. Recently we have shown that activation of PLC by angiotensin II or by other Ca^{2+}-mobilizing agonists reduced the TASK-1 current, an effect probably related to the phosphatidyl-inositol-4,5-bisphosphate (PIP_2) breakdown (17); a similar mechanism for the TASK-3 inhibition would be plausible.

Summarizing our results, the high level expression of TASK-3, the high RR sensitivity of I_{TASK-3}, and its limited inhibition by acidification in the physiological range indicate that TASK-3 is the major determinant of the resting K^+ conductance in glomerulosa cells. This channel, similarly to TASK-1, is inhibited by angiotensin II and, being a target of receptor-mediated regulation, it certainly participates in the complex effect of the hormone.

MATERIALS AND METHODS

Materials

Enzymes and kits for molecular biological studies were purchased from Ambion, Inc. (Austin TX), Amersham Pharmacia Biotech (Little Chalfont, UK), Fermentas (Vilnius, Lithuania), New England Biolabs, Inc. (Beverly, MA), Pharmacia Biotech (Uppsala, Sweden), Promega Corp. (Madison, WI), and Stratagene (La Jolla, CA). Fine chemicals of analytical grade were obtained from Fluka (Buchs, Switzerland), Promega Corp., and Sigma (St. Louis, MO). [α-^{32}P]dCTP was obtained from Izinta (Budapest, Hungary).

RNA Preparation and RT-PCR

Total RNA was prepared from adrenal capsular tissue [mainly glomerulosa cells (13)] by the guanidium-isothiocyanate, phenol-chloroform method as previously described (14). The quantitation of the RNA was based on its absorbance at 260 nm, and its integrity was confirmed by agarose-formaldehyde gel electrophoresis. For PCR total RNA (1 μg) was reverse transcribed by mouse Moloney leukemia virus reverse transcriptase.

For detection of the TASK-3 message in glomerulosa tissue, the forward primer (T3s) was 5′-ggcatATGAAGCGGCAGAAtGTGCG-3′, and the reverse primer (T3a) was 5′-TCCCTCtAGAAGATCTTCATCGGTATT-3′. The sense primer annealed to the start codon region of TASK-3 with one mismatch indicated by *lowercase letter*. (The sequence of TASK-3 is identical with that of TASK-1 in this region apart from this single base difference.) The mismatch in T3s caused a silent mutation, leaving the TASK-3 amino acid sequence unaltered. The antisense primer was specific exclusively for TASK-3. To promote cloning of the PCR product the T3s primer had an additional short sequence at the 5′-end, generating an *Nde*I restriction enzyme recognition site, whereas an *Xba*I restriction enzyme site was introduced into the T3a primer close to its 5′-end. The cDNA was amplified with a PCR protocol of 25 cycles (denaturation for 30 sec at 94 C, annealing for 1 min at 50 C, extension for 90 sec at 72 C) and final extension for 5 min at 72 C.

Cloning of the cDNA Encoding TASK-3

The coding region of TASK-3 was amplified from total glomerulosa RNA using Pfu turbo DNA polymerase after reverse transcription. PCR primers were based on the published rat TASK-3 sequence. The forward primer was T3s (see above); the reverse primer (T3end-a) was 5′-cctctctagACTTAGATGGACTTGCGACG 3′. The additional bases at the 5′-end (indicated by *lowercase letters*) introduced an *Xba*I restriction enzyme site. The PCR product was digested with *Xba*I enzyme and cloned into the *Xba*I-*Sma*I-digested Bluescript pKS-phagemid (Stratagene). Subsequently it was subcloned into pEXO vector containing the 5′- and 3′-untranslated regions of the *Xenopus* globin gene. The sequence of the construct (pEXO-TASK-3) was determined from both directions by automatic sequencing.

Quantification of the mRNA Expression of the Three TASK Channels

To estimate the relative abundance of TASK-1, TASK-2, and TASK-3 mRNA in the glomerulosa tissue, degenerate primers were used to amplify all three messages simultaneously. The forward primer (T123s) 5′-GTCAT(C/T)AC(A/C)AC(T/C)AT(T/C)GG(A/C)TATGG-3′ and the reverse primer (T123a) 5′-A(G/T) (G/T)GT(G/A)ATGAAG(G/C)AGTAGTA-3′ annealed to highly conserved regions (corresponding to the K^+ channel pore forming P1 and P2 segment of each channel), which flanked subtype-specific sequences. This allowed identification of the amplified product by restriction enzyme mapping. The radioactive PCR product [each PCR mixture contained [α-^{32}P]dCTP (50 kBq)] was purified as previously described (14) and divided into aliquots, and the aliquots were digested with *Nco*I, *Pvu*II, and *Eco*91I restriction enzymes, which were specific for the products deriving from TASK-1, TASK-2, and TASK-3, respectively. The digested samples were electrophoretically separated, and the degree of digestion was determined by phosphor imager (model GS-525, Bio-Rad Laboratories, Inc., Hercules, CA).

For obtaining more quantitative data we measured the mRNA levels of the three TASK channels by competitive PCR. The competitive templates for TASK-1 and TASK-3 were the mutant pEXO-TASK-1 (15) and pEXO-TASK-3 plasmids, respectively, in which the *Nco*I (or *Kpn*2I in TASK-3) restriction enzyme site was destroyed by digesting with the respective enzyme, creating blunt ends (Klenow polymerase), and religating. Because the rat TASK-2 cDNA has not yet been cloned, we amplified a fragment of the rat TASK-2 coding region from glomerulosa RNA applying the degenerate AC(C/T)GTCATCAC(A/C)ACCAT(A/C)GG sense, and G(C/G)CAC(A/G)(A/T)AGTCICC(A/G)AAICC(A/T) antisense oligonucleotides. The TASK-2 RT-PCR product was cloned into the *Eco*RV site of Bluescript pKS- (Stratagene), and sequenced. The TASK-2 competitive template was produced by destroying the *Eco*81I restriction enzyme site of this clone. The template regions of the competitive templates were cleaved out from the plasmids (TASK-1, *Hin*fI; TASK-2, *Eco*RI and *Xho*I; TASK-3, *Eco*81I and *Sma*I) to facilitate denaturation. Known amounts of these digested competitive templates were mixed with reverse transcription reactions from 200 ng glomerulosa RNA, and the PCR was performed with the highly thermostable Vent DNA polymerase (initial denaturation for 2 min at 98 C, 30 cycles of denaturation for 30 sec at 98 C, annealing for 1 min at 51 C, extension for 40 sec at 72 C, and final extension for 5 min at 72 C). The primer pairs were specific for the different TASK channels. (TASK-1, GCGTCGTGCTGCGCCTCAAG sense, TCCTTCTGCAGCGCCACGTAG antisense; TASK-2, GGGCGCCTCTTCTGTGTCTTC sense, AGGCCCTCAATGTAGTTCCAC antisense; TASK-3, CTCTGCTTCCCTGGTGCCAAC sense, ATGGACTTGCGACGGATGTGC antisense.) The radioactive TASK-1, TASK-2, and TASK-3 competitive PCR products were digested completely with *Nco*I, *Eco*81I, and *Kpn*2I, respectively. The digested fragments (deriving from the glomerulosa RNA) were separated from the digestion-resistant product (deriving from the competitive template) on agarose gel, and the radioactivity of the bands was measured by phosphor imager. The ion channel mRNA expression level was calculated in moles of competitive template strand per μg of glomerulosa total RNA from the reactions in which the radioactive counts of the digested and digestion-resistant products were nearly equal.

Northern Blot

Ten micrograms of total RNA from different tissues were loaded and run on a 1% agarose formaldehyde gel after denaturation. The electrophoretic separation of RNA was followed by its transfer to Nytran nylon membrane (Schleicher & Schuell, Inc., Keene, NH). For the TASK-3 probe, the *Bgl*II-*Xba*I fragment (440 bp, corresponding to the unique C-terminal intracellular tail of the channel) was labeled with [^{32}P]dCTP (2 MBq) by random primed reaction using the Oligolabeling Kit from Pharmacia Biotech. Hybridization was carried out at 42 C for 24 h. After hybridization the blot was washed successively in buffers of 1× SSPE + 0.1% SDS twice for 30 min at room temperature and 0.1× SSPE + 0.1% SDS twice for 30 min at 70 C. After detection of the radioactivity by phosphor imager, the membrane was stripped and reprobed for glyceraldehyde-3-phosphate dehydrogenase reference signal as previously described (14).

mRNA Purification and cRNA Synthesis

mRNA was purified from total RNA by Dynabeads Oligo $(dT)_{25}$ (DynAl, Oslo, Norway), divided into aliquots, and stored at −70 C. The cRNAs of TASK-1 and TASK-3 potassium channels and AT_{1a} and muscarinic M1 receptors were synthesized *in vitro* according to the manufacturer's instructions (Ambion, Inc. mMESSAGE mMACHINE T7 *In vitro* Transcription Kit). The templates were the *Xba*I-linearized pEXO-TASK-1 (15) and pEXO-TASK-3 constructs, the *Not*I-linearized plasmid comprising the coding sequence and 5′-untranslated region of rat AT1a angiotensin II receptor (a gift from Dr. K. E. Bernstein), and the *Bam*HI-linearized pcDNA3.1 (Invitrogen) containing the coding sequence of the human M1 muscarinic acetylcholine receptor in its *Eco*RI site (a gift from Dr. Xin-Yun Huang).

Animals and Tissue Preparation and *Xenopus laevis* Oocyte Injection

Mature female *X. laevis* frogs were obtained from Amrep Reptielen (Breda, Netherlands). Frogs were anesthetized by immersing them into benzocaine solution (0.03%). Ovarian lobes were removed, the tissue was dissected and treated with collagenase (1.45 mg/ml, 148 U/mg, type I, Worthington Biochemical Corp., Freehold, NJ) and continuous mechanical agitation in Ca^{2+}-free OR2 solution containing (in mM): NaCl, 82.5; KCl, 2; $MgCl_2$, 1; HEPES, 5, pH 7.5) for 1.5–2 h. Stage V and VI oocytes were defolliculated manually and kept at 18 C in modified Barth's saline containing (in mM): NaCl, 88; KCl, 1; $NaHCO_3$, 2.4; $MgSO_4$, 0.82; $Ca(NO_3)_2$, 0.33; $CaCl_2$, 0.41; HEPES, 20; buffered to pH 7.5 with NaOH and supplemented with penicillin (100 U/ml), streptomycin (100 μg/ml), sodium pyruvate (4.5 mM), and theophylline (0.5 mM). Oocytes were injected 1 d after defolliculation. Fifty nanoliters of the appropriate RNA solution were delivered with Nanoliter Injector (World Precision Instruments, Saratosa, FL). Electrophysiological experiments were performed 3 or 4 d after the injection.

The tissues for RNA preparation were derived from Wistar rats (250–350 g), which were stunned before decapitation. All treatment of the animals was conducted in accordance with state laws and institutional regulations. The experiments were approved by the Animal Care and Ethics Committee of Semmelweis University.

Electrophysiology

Membrane currents were recorded by two-electrode voltage clamp (OC-725-C, Warner Instrument Corp., Hamden, CT) using microelectrodes made of borosilicate glass (Clark Electromedical Instruments, Pangbourne, UK) with resistance of 0.3–1 megaohm when filled with 3 M KCl. Currents were filtered at 1 kilohertz, digitally sampled at 1–2.5 kilohertz with a Digidata Interface (Axon Instruments, Foster City, CA), and stored on a PC/AT computer. Recording and data analysis were performed using pCLAMP software 6.0.4 (Axon Instruments). Experiments were carried out at room temperature, and solutions were applied by a gravity-driven perfusion system. Low [K^+] solution contained (in mM): NaCl, 95.4; KCl, 2; $CaCl_2$, 1.8; HEPES, 5. High [K^+] solution contained 80 mM K^+ (78 mM Na^+ of the low [K^+] solution was replaced with K^+). Unless otherwise stated, the pH of every solution was adjusted to 7.5 with NaOH. Perifusing solutions with pH < 6.5 were buffered by including 5 mM 2-[*N*-morpholino]ethane sulphonic acid in addition. Background K^+ currents were measured in high EC [K^+] at the end of 300 msec long voltage steps to −100 mV applied in every 3 sec. The holding potential was 0 mV. Where it was possible, the inward current in high [K^+] was corrected for the small nonspecific leak measured in 2 mM EC [K^+].

Statistics and Calculations

Data are expressed as means ± SEM. Normalized dose-response curves were fitted (least squares method, Sigmaplot, Jandel Corp., San Rafael, CA) to a Hill equation of the form: $y = 1/[1 + (c/K_{1/2})^n]$, where c is the concentration, $K_{1/2}$ is the concentration at which half-maximal inhibition occurs, and n is the Hill coefficient. Where the treatment failed to

cause complete inhibition, a modified form of the equation was used: $y = \alpha/[1 + (c/K_{1/2})^n] + (1 - \alpha)$, where α is the fraction inhibited by the treatment.

Acknowledgments

The authors thank Professor M. Lazdunski and Dr. F. Lesage for the pEXO and pEXO-TASK plasmids and Dr. K. E. Bernstein for the angiotensin II (AT1a) receptor plasmid construct. The skillful technical assistance of Miss Erika Kovács and Mrs. Irén Veres is greatly appreciated.

Received June 25, 2001. Accepted November 20, 2001.

Address all correspondence and requests for reprints to: Peter Enyedi, M.D., Ph.D., Department of Physiology, Semmelweis University of Medicine, P.O Box 259, H-1444 Budapest, Hungary. E-mail: enyedi@puskin.sote.hu.

This work was supported by the Hungarian National Research Fund (OTKA 032159), the Hungarian Medical Research Council (ETT-248/2000) and the Hungarian-French Intergovernmental Scientific & Technological Cooperation Program (TÉT F-34/00).

REFERENCES

1. Vassilev PM, Kanazirska MV, Quinn SJ, Tillotson DL, Williams GH 1992 K^+ channels in adrenal zona glomerulosa cells. I. Characterization of distinct channel types. Am J Physiol 263:E752–E759
2. Brauneis U, Vassilev PM, Quinn SJ, Williams GH, Tillotson DL 1991 ANG II blocks potassium currents in zona glomerulosa cells from rat, bovine, and human adrenals. Am J Physiol 260:E772–E779
3. Payet MD, Durroux T, Bilodeau L, Guillon G, Gallo-Payet N 1994 Characterization of K^+ and Ca^{2+} ionic currents in glomerulosa cells from human adrenal glands. Endocrinology 134:2589–2598
4. Payet MD, Bilodeau L, Drolet P, Ibarrondo J, Guillon G, Gallo-Payet N 1995 Modulation of a Ca^{2+}-activated K^+ channel by angiotensin II in rat adrenal glomerulosa cells: Involvement of a G protein. Mol Endocrinol 9:935–947
5. Lotshaw DP 1997 Characterization of angiotensin II-regulated K^+ conductance in rat adrenal glomerulosa cells. J Membr Biol 156:261–277
6. Lotshaw DP 1997 Effects of K^+ channel blockers on K^+ channels, membrane potential, and aldosterone secretion in rat adrenal zona glomerulosa cells. Endocrinology 138:4167–4175
7. Czirják G, Fischer T, Spät A, Lesage F, Enyedi P 2000 TASK (TWIK-related acid-sensitive K^+ channel) is expressed in glomerulosa cells of rat adrenal cortex and inhibited by angiotensin II. Mol Endocrinol 14:863–874
8. Patel AJ, Honore E 2001 Properties and modulation of mammalian 2P domain K^+ channels. Trends Neurosci 24:339–346
9. Patel AJ, Maingret F, Magnone V, Fosset M, Lazdunski M, Honoré E 2000 TWIK-2, an inactivating 2P domain K^+ channel. J Biol Chem 275:28722–28730
10. Reyes R, Duprat F, Lesage F, Fink M, Salinas M, Farman N, Lazdunski M 1998 Cloning and expression of a novel pH-sensitive two pore domain K^+ channel from human kidney. J Biol Chem 273:30863–30869
11. Kim Y, Bang H, Kim D 2000 TASK-3, a new member of the tandem pore K^+ channel family. J Biol Chem 275: 9340–9347
12. Rajan S, Wischmeyer E, Liu GX, Müller RP, Daut J, Karschin A, Derst C 2000 TASK-3, a novel tandem pore domain acid-sensitive K^+ channel—an extracellular histidine as pH sensor. J Biol Chem 275:16650–16657
13. Giroud CJP, Stachenko J, Venning EH 1956 Secretion of aldosterone by the zona glomerulosa of the rat adrenal glands incubated *in vitro*. Proc Soc Exp Biol Med 92: 154–158
14. Horváth A, Szabadkai G, Várnai P, Arányi T, Wollheim CB, Spät A, Enyedi P 1998 Voltage dependent calcium channels in adrenal glomerulosa cells and in insulin producing cells. Cell Calcium 23:33–42
15. Duprat F, Lesage F, Fink M, Reyes R, Heurteaux C, Lazdunski M 1997 TASK, a human background K^+ channel to sense external pH variations near physiological pH. EMBO J 16:5464–5471
16. Szabadkai G, Várnai P, Enyedi P 1999 Selective inhibition of potassium-stimulated rat adrenal glomerulosa cells by ruthenium red. Biochem Pharmacol 57:209–218
17. Czirják G, Petheõ, Spät A, Enyedi P 2001 Inhibition of TASK1 potassium channel by phospholipase C. Am J Physiol 281:C700–C708
18. Decher N, Maier M, Dittrich W, Gassenhuber J, Bruggemann A, Busch AE, Steinmeyer K 2001 Characterization of TASK-4, a novel member of the pH-sensitive, two-pore domain potassium channel family. FEBS Lett 492: 84–89
19. Cibulsky SM, Sather WA 1999 Block by ruthenium red of cloned neuronal voltage-gated calcium channels. J Pharmacol Exp Ther 289:1447–1453
20. Hirano M, Imaizumi Y, Muraki K, Yamada A, Watanabe M 1998 Effects of ruthenium red on membrane ionic currents in urinary bladder smooth muscle cells of the guinea-pig. Pflugers Arch 435:645–653
21. Amann R, Maggi CA 1991 Ruthenium red as a capsaicin antagonist. Life Sci 49:849–856
22. Lin MJ, Lin-Shiau SY 1996 Ruthenium red, a novel enhancer of K^+ currents at mouse motor nerve terminals. Neuropharmacology 35:615–623
23. Cohen CJ, McCarthy RT, Barrett PQ, Rasmussen H 1988 Ca^{2+} channels in adrenal glomerulosa cells: K^+ and angiotensin II increase T-type Ca^{2+} channel current. Proc Natl Acad Sci USA 85:2412–2416
24. Quinn SJ, Brauneis U, Tillotson DL, Cornwall MC, Williams GH 1992 Calcium channels and control of cytosolic calcium in rat and bovine zona glomerulosa cells. Am J Physiol 262:C598–C606
25. Balla T, Várnai P, Holló Z, Spät A 1990 Effects of high potassium concentration and dihydropyridine Ca^{2+}-channel agonists on cytoplasmic Ca^{2+} and aldosterone production in rat adrenal glomerulosa cells. Endocrinology 127:815–822
26. Chen XL, Bayliss DA, Fern RJ, Barrett PQ 1999 A role for T-type Ca^{2+} channels in the synergistic control of aldosterone production by ANG II and K^+. Am J Physiol 276:F674–F683
27. Durroux T, Gallo-Payet N, Payet MD 1988 Three components of the calcium current in cultured glomerulosa cells from rat adrenal gland. J Physiol (Lond) 404: 713–729
28. Schrier AD, Wang H, Talley EM, Perez-Reyes E, Barrett PQ 2001 α1H T-type Ca^{2+} channel is the predominant subtype expressed in bovine and rat zona glomerulosa. Am J Physiol 280:C265–C272
29. Rossier MF, Burnay MM, Vallotton MB, Capponi AM 1996 Distinct functions of T- and L-type calcium channels during activation of bovine adrenal glomerulosa cells. Endocrinology 137:4817–4826
30. Yingst DR, Davis J, Schiebinger R 2001 Effects of extracellular calcium and potassium on the sodium pump of rat adrenal glomerulosa cells. Am J Physiol 280: C119–C125